Cavity-Enabled Real-Time Observation of Individual Atomic Collisions

Matthew L. Peters,[1,2,*] Guoqing Wang (王国庆),[1,2,*] David C. Spierings,[1,2,*] Niv Drucker,[3] Beili Hu,[1,2] Meng-Wei Chen,[1,2] Yu-Ting Chen,[1,2,4,†] and Vladan Vuletić[1,2,‡]

[1]*MIT-Harvard Center for Ultracold Atoms and Research Laboratory of Electronics, Massachusetts Institute of Technology, Cambridge, Massachusetts 02139, USA*

[2]*Department of Physics, Massachusetts Institute of Technology, Cambridge, Massachusetts 02139, USA*

[3]*Quantum Machines, Tel Aviv-Yafo 6721407, Israel*

[4]*Department of Physics, Harvard University, 17 Oxford Street, Cambridge, Massachusetts 02138, USA*

(Received 19 November 2024; accepted 30 July 2025; published 26 August 2025)

Using the strong dispersive coupling to a high-cooperativity cavity, we demonstrate fast and nondestructive number-resolved detection of atoms in optical tweezers. We observe individual atom-atom collisions, quantum state jumps, and atom loss events with a time resolution of 100 μs through continuous measurement of cavity transmission. Using adaptive feedback control in combination with the nondestructive measurements, we further prepare a single atom with 92(2)% probability.

DOI: 10.1103/941q-5sdq

Arrays of individual neutral atoms represent a promising platform for quantum information processing due to their scalability, arbitrary connectivity, and long coherence times [1–3]. These features are enabled in large part by the simple trapping and high-fidelity fluorescence imaging of individual atoms within tweezer traps. While the fluorescence imaging onto a camera has the advantage of parallelism, i.e., many traps can be imaged simultaneously, the imaging time is limited by the effective photon collection efficiency of free-space optics, which is typically 1%–2% [1].

Atom detection via a cavity [4,5] offers the advantage that the signal-to-noise ratio can exceed that of an ideal 4π fluorescence detector, enabling much faster detection and thereby observation of real-time single atom dynamics [6–12]. The tight optical confinement of nanofibers has also enabled atom detection [13,14] in real time [15]. Furthermore, the cavity has been utilized for high-fidelity state discrimination [16–19]. These capabilities, among others, have motivated much recent work on tweezer integration [20–26], as well as many other experiments coupling cold atoms and cavities [27–29].

While most experiments have employed the simpler standing-wave cavities, ring cavities [30–35] supporting travelling-wave eigenmodes have the advantage of nearly uniform atom-mode coupling along the mode. Bow-tie ring cavities [36,37] enable small foci and strong light-matter interactions while maintaining large optical access, making them ideal for integration with tweezer arrays [24,38]. Such systems have previously been used for the real-time detection of a few atoms [39–41], and for studies of ensemble dynamics [42–44].

In this Letter, we demonstrate fast, nondestructive, state- and number-resolving measurements enabled by a high-cooperativity ring cavity [24,38]. The strong atom-light coupling [cooperativity $\eta = 21.0(3)$] gives rise to large dispersive cavity shifts by individual atoms even far from atomic resonance, which is used to distinguish different numbers of atoms in a single dipole trap or small tweezer array. With a time resolution of 100 μs, we directly observe for the first time individual inelastic light-induced collisions [45,46] between pairs of atoms in an optical tweezer, which represents the mechanism that underpins the loading of at most one atom into a tweezer [47–50]. We also demonstrate a protocol that uses cavity measurement and adaptive feedback to realize quasideterministic loading of a single atom with 92(2)% fidelity.

Figure 1 illustrates the experimental setup. Cold Cs atoms are prepared in a magneto-optical trap (MOT) near the center of an in-vacuum bow-tie ring cavity, which has a round-trip length of 18.6 cm, a waist of $w_c = 7$ μm, and a finesse of $\mathcal{F} = 50\,000$ [38]. The atoms are loaded directly from the MOT into a one-dimensional array of optical tweezers at a temperature of ∼50 μK, measured via release and recapture. The traps are created by 937-nm light, which is magic on the D_2 transition and thus enables homogeneous coupling of near resonant light across the array [51–53]. The tweezer traps are generated by an acousto-optic deflector, and focused by an out-of-vacuum microscope objective (numerical aperture $NA = 0.5$) to waists of $w = 1.0$ μm with a trap depth $U/h = 24$ MHz and radial trapping frequency $\omega_r/(2\pi) = 85$ kHz. The hyperfine state of the atoms is controlled by applying 'repumping' and

[*]These authors contributed equally to this work.

[†]Present Address: Institute for Quantum Computing and Department of Physics and Astronomy, University of Waterloo, Waterloo, Ontario N2L 3G1, Canada.

[‡]Contact author: vuletic@mit.edu

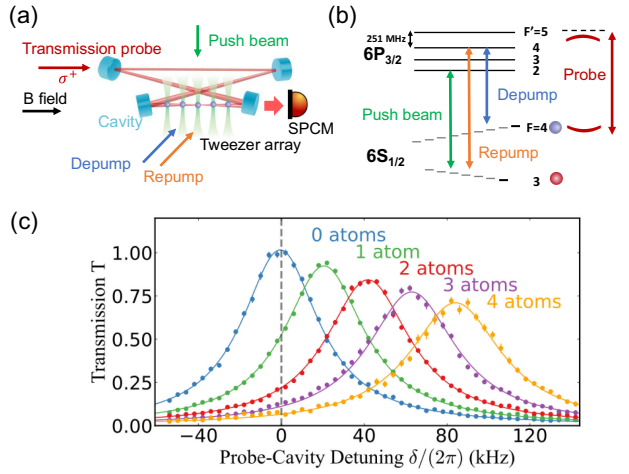

FIG. 1. Experimental configuration. (a) Schematic of the experimental setup. Cesium atoms in optical tweezers are positioned within a bow-tie running-wave cavity. (b) Relevant level structure of Cs atoms. (c) Cavity transmission spectrum for 0 (blue), 1 (green), 2 (red), 3 (purple), and 4 (orange) atoms trapped within the cavity. Here the cavity is blue-detuned by $\Delta/(2\pi) = +50$ MHz from the $|F = 4\rangle$ to $|F' = 5\rangle$ component of the D_2 line.

'depumping' light on the $|6S_{1/2}, F = 3\rangle \rightarrow |6P_{3/2}, F' = 4\rangle$ and $|6S_{1/2}, F = 4\rangle \rightarrow |6P_{3/2}, F' = 4\rangle$ hyperfine transitions, respectively.

We calibrate the strength of the atom-cavity coupling via the dispersive shift of the cavity resonance by individual atoms. Single atoms are prepared in the tweezer traps by a brief stage of polarization gradient cooling. This induces light-assisted collisions, leaving each tweezer with an occupation of zero or one atom [54]. We apply a magnetic field of 5.3(1) G along the cavity axis and probe the dispersive shift. Figure 1(c) shows the measured cavity transmission for different numbers of individually trapped atoms, where the atom number is determined independently by imaging the atoms through the microscope objective onto a camera. For the data in Fig. 1(c), the cavity (frequency ω_c) is blue-detuned from the atomic $|F = 4\rangle \rightarrow |F' = 5\rangle$ resonance (frequency ω_a) by $\Delta = \omega_c - \omega_a = +2\pi \times 50$ MHz, and the probe-cavity detuning $\delta = \omega_p - \omega_c$ is varied.

We note that a distinguishing characteristic of our cavity is that a small deviation of the cavity geometry from planar leads to (near)-circularly polarized cavity modes [36,55,56] that are split by 8.4 MHz. We probe the cavity transmission using the σ^+ polarized mode in the clockwise direction. Backscattering into the degenerate frequency σ^- mode is eliminated when the atom is pumped into the stretched state, and backscattering into the counterpropagating σ^+ mode is far detuned. Atoms therefore only forward scatter light into the same clockwise σ^+ polarized mode.

The single-atom cooperativity for coupling to the TEM_{00} mode, $\eta = 21.0(3)$, is extracted from a simultaneous fit of all the data to the transmission [57]

$$T = \frac{1}{\left(1 + N\eta\frac{1}{1+y^2}\right)^2 + \left(x - N\eta\frac{y}{1+y^2}\right)^2}, \tag{1}$$

where N is the atom number in the cavity, $y = 2(\omega_p - \omega_a)/\Gamma$ and $x = 2(\omega_p - \omega_c)/\kappa$ are the normalized probe-atom detuning and probe-cavity detuning, where $\Gamma/(2\pi) = 5.2$ MHz and $\kappa/(2\pi) = 37$ kHz are the atomic and cavity linewidths, respectively.

We operate in the dispersive regime of cavity probing ($N\eta/(1 + y^2) < 1$), where the atomic absorption is small. For the cavity probe fixed on the empty-cavity resonance ($\delta = 0$), we observe a significantly shorter trap lifetime during probing for red detuning with $\Delta < 0$ (~6 ms) than for blue detuning with $\Delta > 0$ (~50 ms). For $\delta = 0$, cavity cooling (heating) occurs when $\Delta > 0$ ($\Delta < 0$) [58,59]. Cavity cooling typically occurs through backscattering of photons which yields the largest momentum transfer [60], but this is suppressed in our cavity. Instead, cooling results from strong modulation of photon number in the cavity due to atomic motion [61] in the tightly focused cavity mode. As an atom moves through the cavity, it experiences a potential that derives from the ac stark shift of the intracavity light. This potential is maximum for a stationary atom at the center of the cavity mode, and equal in magnitude to the dispersive shift observed in Fig. 1(c) multiplied by the intracavity photon number. The atom's axial motion in the tweezer, transverse to the cavity mode, modulates the intracavity photon number and the light shift experienced by the atom, with a delay time given by the ringdown time ($\tau = 4.3$ μs) of the cavity. This leads to a Sisyphus-like effect that cools atoms when $\Delta > 0$ with a timescale of ~10 ms [62]. This cavity cooling mechanism has been observed in a standing-wave cavity [63] and a detailed description of the light forces at play has been obtained [64–66]. To observe the atoms while also cooling them, we operate at blue light-atom detuning of $\Delta/(2\pi) = 107$ MHz, where the transmission is sufficiently atom-number dependent to allow us to resolve 0, 1, 2, 3, and 4 atoms within a typical measurement time of 100 μs.

Figure 2(a) shows the histogram of the measured cavity transmission T, which is normalized by the empty-cavity transmission level. We observe pronounced peaks corresponding to different atom numbers inside the cavity. Those peaks provide a calibration of atom number when we observe individual time traces displaying real-time atomic dynamics, where the short-dashed lines are extracted from the peak positions and the long-dashed lines are extrapolated from the measured cooperativity. (For atoms trapped in an intracavity lattice, similar continuous-time signals were first observed in Ref. [40], while Ref. [67] observed quantum jumps out of Rydberg levels that may have arisen from light-assisted collisions.) Figure 2(b) shows characteristic time traces when we probe

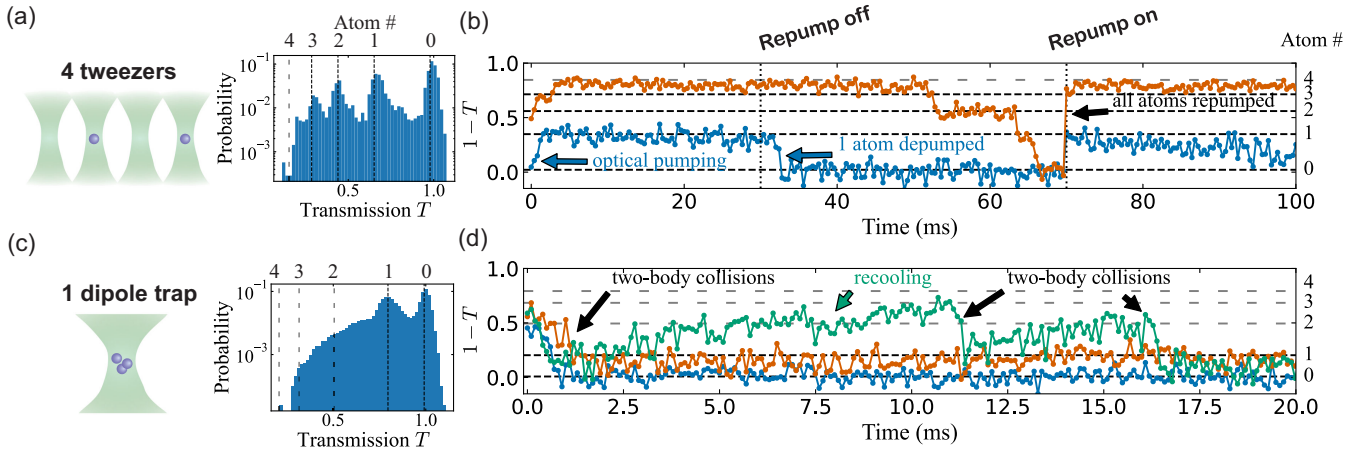

FIG. 2. Real-time measurement of atom dynamics. The cavity is blue-detuned by $\Delta/(2\pi) = 107$ MHz from atomic $|F = 4\rangle \rightarrow |F = 5\rangle$ resonance while the probe is resonant with the empty cavity ($\delta = 0$). (a) Histogram of the probability for cavity transmission in 400-μs bins for single atoms probabilistically loaded into four separate tweezers (waist $w = 1.0$ μm). Peaks in the distribution are associated with atom numbers. (b) A measure of atom-cavity coupling $1 - T$ for cavity transmission T, from the dataset in (a). Representative time traces showcase atom number resolution, as well as quantum jumps associated with optical pumping between the hyperfine ground states $F = 3$, 4. In these measurements, the average intracavity photon number without any atoms is 8. (c),(d) Measurements as in (a),(b), but for several atoms initially loaded into a slightly bigger dipole trap (waist $w = 1.4$ μm) with 100-μs bins. Inelastic collisions cause heating or trap loss and decrease the coupling. Here the average empty intracavity photon number is 38.

the cavity coupling $1 - T$ after probabilistic loading of four separate tweezers, each containing at most one atom. The steplike time traces in Fig. 2(b) display quantum jumps [68] associated with the optical pumping of individual atoms between hyperfine ground states, since only atoms in the manifold $|F = 4\rangle$ are strongly coupled to the cavity mode. The total atom number is measured by turning on the repumping light that transfers all atoms to the $|F = 4\rangle$ manifold. At the beginning of each trace, we observe a fast decrease in transmission, with a measured time constant of 1.1(0.2) ms, corresponding to the optical pumping of atoms to the $|F = 4, m_F = 4\rangle$ magnetic sublevel, for which the coupling to the circularly polarized cavity mode is maximized.

Having calibrated and verified the atom-number-dependent transmission, we then proceed to probe the dynamics of several atoms in a single trap [Fig. 2(c)]. By removing the polarization gradient cooling from the loading procedure and slightly enlarging the trap waist size to $w = 1.4$ μm [trap depth $U/h = 22$ MHz, radial trapping frequency $\omega_r/(2\pi) = 58$ kHz, and axial frequency $\omega_{ax}/(2\pi) = 8.8$ kHz], we load multiple atoms into a single dipole trap. In the larger trap the atomic density and rate of light-induced two-body collisions are sufficiently reduced to become observable by the cavity measurement. Figure 2(d) shows multi-atom time traces that display random large and abrupt transmission changes consistent with collisional loss and collisional heating induced by binary atomic collisions within the single trap. We observe that when the trap initially contains two atoms, a collision event often leaves the trap empty, while a collision in a sample of three atoms often results in a single, stably trapped atom. We conclude that we are observing the real-time collisional dynamics upon which single-atom tweezer loading relies [50,54]. Light-assisted collisional loss should occur near-instantaneously compared to our timing resolution. This is often observed in our measurements after $\gtrsim 1$ ms of cavity probing (see Ref. [62] for additional traces). Some traces show slower dynamics that may arise from multiple collisions between hotter atoms in the trap, though shot noise can make it challenging to conclusively resolve multiple near-simultaneous collisions.

We also observe instances of collisions that result in temporarily reduced coupling, but not in the ejection of atoms from the dipole trap. For example, the green trace in Fig. 2(d) shows a sharp decrease of coupling $1 - T$ at $t_1 = 1$ ms, followed by a gradual increase of the atom-cavity coupling back to the value prior to the abrupt change. We interpret this behavior as representing a collision that imparts a significant amount of kinetic energy to the atoms, though insufficient to eject them from the trap. Atoms with a high kinetic energy following an inelastic collision are displaced further from the center of the cavity mode (waist $w_c = 7$ μm), and more weakly coupled. As cavity cooling reduces the atomic temperature, the coupling slowly increases, as observed in the green trace for times between 2 and 11 ms, before two more inelastic collision events, one at $t_2 = 11.5$ ms and one at $t_3 = 16.5$ ms, expel two atoms, and leave just one atom remaining in the trap. (We observe that single atoms remain trapped for long times, with no significant changes in coupling.) As a consequence of the changes of transmission due to collisions and recooling, the histogram for several atoms in a single trap, Fig. 2(c), only displays two peaks, corresponding to the stable traces for

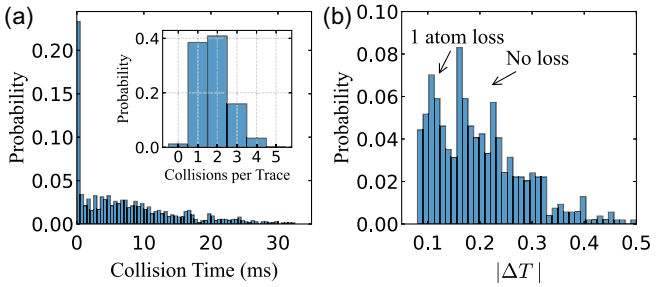

FIG. 3. Analysis of atomic collisions. (a) Probability distribution of the collision times from time traces as in Fig. 2(d). Several atoms are loaded at $t = 0$ into a single dipole trap. We identify atomic collisions as abrupt increases in transmission that correspond to an apparent loss of more than one atom. The inset shows the number of observed atomic collisions before a steady state with zero or one atoms is reached. (b) Histogram of the slow increase in cavity coupling $1 - T$ that follows 50% of the detected atomic collisions. We observe a peak consistent with retention of one atom after collisions ($|\Delta T| \sim 0.12$), as well as greater increases in coupling ($|\Delta T| > 0.15$) indicating no loss of atoms. Changes $|\Delta T| \leq 7\%$ are consistent with shot noise and not considered.

zero and one atoms. In a separate, single-atom measurement [62], we have measured a time constant for recoupling of an atom to the cavity after significant heating of (11 ± 3) ms, consistent with the above explanation for cooling. We note that optical pumping between magnetic sublevels [see Fig. 2(b)], which can also lead to increased cavity coupling, occurs on a faster (∼1 ms) timescale.

We further analyze the collisional dynamics and summarize our findings in Fig. 3. Our data reveal that 20% of the observed collisions occur within the first 100 μs of cavity probing, while the remaining collisions occur over a much longer timescale with an average of ∼9 ms as shown in Fig. 3(a). We attribute the fast initial collision rate as being due to a larger atomic density immediately after trap loading. The longer timescale probably arises from multiple axial oscillations along the tweezer, where two atoms interacting in the presence of light via the resonant dipole-dipole interaction, with a collision cross section $\sigma \approx [\lambda/(2\pi)]^2$ [45,46] with $\lambda = 852$ nm. The inset in Fig. 3(a) displays the number of collisions observed per experimental cycle before we end up with zero or one atoms. For our conditions, on average 1.8 collisions are needed to reduce the atom number to zero or one. Using a semiclassical model [45,46,48], we estimate an average time between collisions of 35 ms for two atoms at 50 μK in this trapping configuration [62], in reasonable agreement with our observations.

Our data can also be used to characterize the amount of heating in an individual inelastic light-induced collision. As described above, we observe time traces that correspond to two types of collisions: traces with a sudden decrease in coupling to a new constant level can be associated with the colliding atoms leaving the trap, while traces with a sudden decrease followed by a slow increase in cavity coupling, either to the original level or to a lower level, can be attributed to one or both atoms remaining in the trap and being recooled to the cavity mode center. Figure 3(b) quantifies this increase in cavity coupling that often follows a collision: the distribution of coupling increases shows distinct peaks. For instance, when only a small amount of coupling (∼10%) is regained after a collision, we interpret this to indicate that one of the colliding atoms has left the trap, whereas a larger coupling gain likely indicates the retention and recooling of both atoms. We find that about half of the observed collisions are followed by an increase in cavity coupling, suggesting the retention of one or both atoms, while the other half of the observed collisions correspond to the loss of both atoms. The sum of the probabilities below $|\Delta T| < 0.15$ in Fig. 3(b) provides an upper-bound of ∼15% probability to lose only one atom after a collision. Collisions that result in the loss of only one atom are known to result in an average loading probability for one atom of over 50% [69–72]. In our experiment, collisional blockade loads a single atom 55% of the time, consistent with only a slight bias from the single atom retention. From the semiclassical model for collisions, we expect 27% of collisions to impart energy less than the trap depth [62], consistent with the observation of Fig. 3(b) that ∼35% of collisions retain both atoms.

Finally, we implement a cavity-measurement-based adaptive feedback protocol for quasideterministic loading of a single atom starting with a small ensemble prepared in the $F = 3$ manifold. A weak repump pulse transfers atoms into $F = 4$ manifold and the atom number in $F = 4$ is probed intermittently via the cavity. Once a single atom is repumped, an intense laser beam tuned to the $|F = 3\rangle \rightarrow |F' = 2\rangle$ transition is applied to push out the remaining atoms. The magnetic fields and laser polarization of the push beam are chosen to minimize the role of a dark state [62].

Figures 4(a) and 4(b) show the performance of the adaptive procedure when preparing a single atom starting from several atoms in four tweezers and in a single dipole trap, respectively. The multitrap and single-trap datasets use atomic detuning of $\Delta/(2\pi) = -73$ and -58 MHz, respectively, in order to more clearly distinguish cavity transmission for one atom from that for other atom numbers.

To avoid trivial procedures where we start and end with one atom or no atom at all, we postselect the datasets on having an initial atom number greater than or equal to 2, as measured by the cavity transmission at the end of the initial optical pumping. The success probability of the adaptive procedure is 92(2)%, with an average time to success of about 15 ms, both when loading from four tweezers and from a single trap. The similar performance of the adaptive protocol in these two cases demonstrates that the pulsed interrogation protocol can minimize collisional loss.

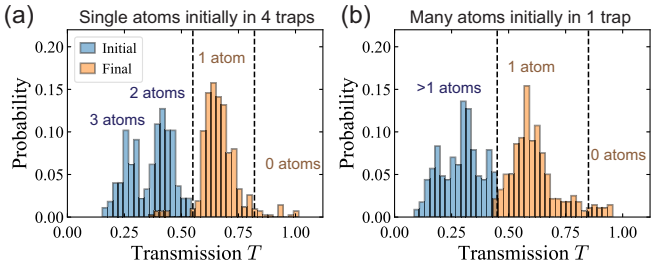

FIG. 4. Adaptive loading of a single atom. The probability to successfully load a single atom in the adaptive protocol (see text) is demonstrated for initial loading of at least two atoms in (a) four tweezer traps [275 trials, $\Delta/(2\pi) = -73$ MHz] and (b) one dipole trap (228 trials, $\Delta/(2\pi) = -58$ MHz). Both datasets had on average 9 intracavity photons when no atoms were present. The initial transmission histogram is shown in blue, while the orange histogram shows the final transmission. The two dashed lines set the threshold for the single-atom transmission. Final-transmission data falling outside the threshold correspond to failures due to atom loss, ejection errors, or reaching the limit of 50 attempts.

The success of the protocol is limited by the incomplete ejection of atoms in the $F = 3$ manifold [62]. We estimate that with improved ejection, as has been demonstrated in [73–76], the protocol could have attained success probabilities of 99%.

The techniques demonstrated here could be expanded in several directions. Adaptive feedback can be combined with machine learning to enhance speed and efficiency [77,78]. Parallelized, near-deterministic loading of single atoms in cavity arrays could circumvent tweezer rearrangement [79,80], which currently is much slower for large arrays than the millisecond timescale for success demonstrated here. Dynamic adjustment of the atomic detuning in our protocol could allow for studies of molecular formation [50,81]. Adaptive feedback also holds promise for mid-circuit operations for quantum computation [18,21,82–86]. Future implementations of adaptive protocols could improve performance using cavities optimized for readout speed, by shortening the cavity length to increase the linewidth.

In summary, we have realized nondestructive atom counting in real-time through measurements of cavity transmission using a high-cooperativity bow-tie cavity. This measurement enables continuous, time-resolved probing of two-body collisional dynamics of atoms within the same trap. Our Letter opens up many new opportunities from the fundamental atomic physics of cold atom collisions and chemical reactions to advancements of neutral-atom quantum information processors.

Acknowledgments—This work is supported by the U.S. Department of Energy, Office of Science, National Quantum Information Science Research Centers, Quantum Systems Accelerator. Additional support is acknowledged from the NSF Frontier Center for Ultracold Atoms (Grant No. PHY-2317134), the NSF QLCI Q-SEnSE (Grant No. QLCI-2016244), and the DARPA ONISQ programme (Grant No. 134371-5113608). We acknowledge Josiah Sinclair, Edita Bytyqi, Gefen Baranes, and Michelle Chong for discussions of light-assisted collisions observed via cavities. The authors thank Alyssa Rudelis, Neng-Chun (Allen) Chiu, Michel Szurek, and Simone Colombe for initial work in constructing the experimental apparatus. We additionally thank Berk Kovos and Christian Hahn for their help in discussing integrating Quantum Machines OPX+ devices into our setup.

[1] H. J. Manetsch, G. Nomura, E. Bataille, K. H. Leung, X. Lv, and M. Endres, A tweezer array with 6100 highly coherent atomic qubits, arXiv:2403.12021.
[2] D. Bluvstein, H. Levine, G. Semeghini, T. T. Wang, S. Ebadi, M. Kalinowski, A. Keesling, N. Maskara, H. Pichler, M. Greiner, V. Vuletić, and M. D. Lukin, A quantum processor based on coherent transport of entangled atom arrays, Nature (London) **604**, 451 (2022).
[3] D. Bluvstein *et al.*, Logical quantum processor based on reconfigurable atom arrays, Nature (London) **626**, 58 (2024).
[4] R. J. Thompson, G. Rempe, and H. J. Kimble, Observation of normal-mode splitting for an atom in an optical cavity, Phys. Rev. Lett. **68**, 1132 (1992).
[5] J. Goldwin, M. Trupke, J. Kenner, A. Ratnapala, and E. A. Hinds, Fast cavity-enhanced atom detection with low noise and high fidelity, Nat. Commun. **2**, 418 (2011).
[6] H. Mabuchi, Q. A. Turchette, M. S. Chapman, and H. J. Kimble, Real-time detection of individual atoms falling through a high-finesse optical cavity, Opt. Lett. **21**, 1393 (1996).
[7] C. J. Hood, M. S. Chapman, T. W. Lynn, and H. J. Kimble, Real-time cavity qed with single atoms, Phys. Rev. Lett. **80**, 4157 (1998).
[8] P. Münstermann, T. Fischer, P. Maunz, P. W. H. Pinkse, and G. Rempe, Dynamics of single-atom motion observed in a high-finesse cavity, Phys. Rev. Lett. **82**, 3791 (1999).
[9] P. W. H. Pinkse, T. Fischer, P. Maunz, and G. Rempe, Trapping an atom with single photons, Nature (London) **404**, 365 (2000).
[10] C. J. Hood, T. W. Lynn, A. C. Doherty, A. S. Parkins, and H. J. Kimble, The atom-cavity microscope: Single atoms bound in orbit by single photons, Science **287**, 1447 (2000).
[11] M. Terraciano, R. Olson Knell, D. Norris, J. Jing, A. Fernández, and L. Orozco, Photon burst detection of single atoms in an optical cavity, Nat. Phys. **5**, 480 (2009).
[12] K. P. Nayak, J. Wang, and J. Keloth, Real-time observation of single atoms trapped and interfaced to a Nanofiber cavity, Phys. Rev. Lett. **123**, 213602 (2019).
[13] E. Vetsch, D. Reitz, G. Sagué, R. Schmidt, S. T. Dawkins, and A. Rauschenbeutel, Optical interface created by laser-cooled atoms trapped in the evanescent field surrounding an optical nanofiber, Phys. Rev. Lett. **104**, 203603 (2010).

[14] A. Goban, K. S. Choi, D. J. Alton, D. Ding, C. Lacroûte, M. Pototschnig, T. Thiele, N. P. Stern, and H. J. Kimble, Demonstration of a state-insensitive, compensated nanofiber trap, Phys. Rev. Lett. **109**, 033603 (2012).
[15] T. Aoki, B. Dayan, E. Wilcut, W. P. Bowen, A. S. Parkins, T. Kippenberg, K. Vahala, and H. Kimble, Observation of strong coupling between one atom and a monolithic microresonator, Nature (London) **443**, 671 (2006).
[16] A. D. Boozer, A. Boca, R. Miller, T. E. Northup, and H. J. Kimble, Cooling to the ground state of axial motion for one atom strongly coupled to an optical cavity, Phys. Rev. Lett. **97**, 083602 (2006).
[17] R. Gehr, J. Volz, G. Dubois, T. Steinmetz, Y. Colombe, B. L. Lev, R. Long, J. Estève, and J. Reichel, Cavity-based single atom preparation and high-fidelity hyperfine state readout, Phys. Rev. Lett. **104**, 203602 (2010).
[18] J. Bochmann, M. Mücke, C. Guhl, S. Ritter, G. Rempe, and D. L. Moehring, Lossless state detection of single neutral atoms, Phys. Rev. Lett. **104**, 203601 (2010).
[19] J. Volz, R. Gehr, G. Dubois, J. Estève, and J. Reichel, Measurement of the internal state of a single atom without energy exchange, Nature (London) **475**, 210 (2011).
[20] T. Dordević, P. Samutpraphoot, P. L. Ocola, H. Bernien, B. Grinkemeyer, I. Dimitrova, V. Vuletić, and M. D. Lukin, Entanglement transport and a nanophotonic interface for atoms in optical tweezers, Science **373**, 1511 (2021).
[21] E. Deist, Y.-H. Lu, J. Ho, M. K. Pasha, J. Zeiher, Z. Yan, and D. M. Stamper-Kurn, Mid-circuit cavity measurement in a neutral atom array, Phys. Rev. Lett. **129**, 203602 (2022).
[22] Y. Liu, Z. Wang, P. Yang, Q. Wang, Q. Fan, S. Guan, G. Li, P. Zhang, and T. Zhang, Realization of strong coupling between deterministic single-atom arrays and a high-finesse miniature optical cavity, Phys. Rev. Lett. **130**, 173601 (2023).
[23] Z. Yan, J. Ho, Y.-H. Lu, S. J. Masson, A. Asenjo-Garcia, and D. M. Stamper-Kurn, Superradiant and subradiant cavity scattering by atom arrays, Phys. Rev. Lett. **131**, 253603 (2023).
[24] X. Zhang, Z. Yu, H. Zhang, D. Xiang, and H. Zhang, Cavity dark mode mediated by atom array without atomic scattering loss, Phys. Rev. Res. **6**, L042026 (2024).
[25] L. Hartung, M. Seubert, S. Welte, E. Distante, and G. Rempe, A quantum-network register assembled with optical tweezers in an optical cavity, Science **385**, 179 (2024).
[26] B. Grinkemeyer, E. Guardado-Sanchez, I. Dimitrova, D. Shchepanovich, G. E. Mandopoulou, J. Borregaard, V. Vuletić, and M. D. Lukin, Error-detected quantum operations with neutral atoms mediated by an optical cavity, Science **387**, 1301 (2025).
[27] H. Ritsch, P. Domokos, F. Brennecke, and T. Esslinger, Cold atoms in cavity-generated dynamical optical potentials, Rev. Mod. Phys. **85**, 553 (2013).
[28] A. Reiserer and G. Rempe, Cavity-based quantum networks with single atoms and optical photons, Rev. Mod. Phys. **87**, 1379 (2015).
[29] F. Mivehvar, F. Piazza, T. Donner, and H. Ritsch, Cavity QED with quantum gases: New paradigms in many-body physics, Adv. Phys. **70**, 1 (2021).
[30] D. Kruse, C. von Cube, C. Zimmermann, and Ph. W. Courteille, Observation of lasing mediated by collective atomic recoil, Phys. Rev. Lett. **91**, 183601 (2003).
[31] J. Klinner, M. Lindholdt, B. Nagorny, and A. Hemmerich, Normal mode splitting and mechanical effects of an optical lattice in a ring cavity, Phys. Rev. Lett. **96**, 023002 (2006).
[32] D. Schmidt, H. Tomczyk, S. Slama, and C. Zimmermann, Dynamical Instability of a Bose-Einstein Condensate in an Optical Ring Resonator, Phys. Rev. Lett. **112**, 115302 (2014).
[33] S. K. Ruddell, K. E. Webb, I. Herrera, A. S. Parkins, and M. D. Hoogerland, Collective strong coupling of cold atoms to an all-fiber ring cavity, Optica **4**, 576 (2017).
[34] D. S. Naik, G. Kuyumjyan, D. Pandey, P. Bouyer, and A. Bertoldi, Bose-einstein condensate array in a malleable optical trap formed in a traveling wave cavity, Quantum Sci. Technol. **3**, 045009 (2018).
[35] S. C. Schuster, P. Wolf, S. Ostermann, S. Slama, and C. Zimmermann, Supersolid properties of a Bose-Einstein condensate in a ring resonator, Phys. Rev. Lett. **124**, 143602 (2020).
[36] N. Jia, N. Schine, A. Georgakopoulos, A. Ryou, A. Sommer, and J. Simon, Photons and polaritons in a broken-time-reversal nonplanar resonator, Phys. Rev. A **97**, 013802 (2018).
[37] X. Li, Y. Zhou, and H. Zhang, Tunable atom-cavity interactions with configurable atomic chains, Phys. Rev. Appl. **21**, 044028 (2024).
[38] Y.-T. Chen, M. Szurek, B. Hu, J. de Hond, B. Braverman, and V. Vuletić, High finesse bow-tie cavity for strong atom-photon coupling in Rydberg arrays, Opt. Express **30**, 37426 (2022).
[39] J. A. Sauer, K. M. Fortier, M. S. Chang, C. D. Hamley, and M. S. Chapman, Cavity QED with optically transported atoms, Phys. Rev. A **69**, 051804(R) (2004).
[40] J. McKeever, J. R. Buck, A. D. Boozer, A. Kuzmich, H.-C. Nägerl, D. M. Stamper-Kurn, and H. J. Kimble, State-insensitive cooling and trapping of single atoms in an optical cavity, Phys. Rev. Lett. **90**, 133602 (2003).
[41] J. McKeever, J. R. Buck, A. D. Boozer, and H. J. Kimble, Determination of the number of atoms trapped in an optical cavity, Phys. Rev. Lett. **93**, 143601 (2004).
[42] K. Baumann, C. Guerlin, F. Brennecke, and T. Esslinger, Dicke quantum phase transition with a superfluid gas in an optical cavity, Nature (London) **464**, 1301 (2010).
[43] R. M. Kroeze, Y. Guo, and B. L. Lev, Dynamical spin-orbit coupling of a quantum gas, Phys. Rev. Lett. **123**, 160404 (2019).
[44] K. Roux, V. Helson, H. Konishi, and J. P. Brantut, Cavity-assisted preparation and detection of a unitary fermi gas, New J. Phys. **23**, 043029 (2021).
[45] K. Burnett, P. S. Julienne, and K.-A. Suominen, Laser-driven collisions between atoms in a Bose-Einstein condensed gas, Phys. Rev. Lett. **77**, 1416 (1996).
[46] K. M. Jones, E. Tiesinga, P. D. Lett, and P. S. Julienne, Ultracold photoassociation spectroscopy: Long-range molecules and atomic scattering, Rev. Mod. Phys. **78**, 483 (2006).
[47] P. Sompet, A. V. Carpentier, Y. H. Fung, M. McGovern, and M. F. Andersen, Dynamics of two atoms undergoing

light-assisted collisions in an optical microtrap, Phys. Rev. A **88**, 051401(R) (2013).
[48] A. Fuhrmanek, R. Bourgain, Y. R. P. Sortais, and A. Browaeys, Light-assisted collisions between a few cold atoms in a microscopic dipole trap, Phys. Rev. A **85**, 062708 (2012).
[49] S. D. Gensemer and P. L. Gould, Ultracold collisions observed in real time, Phys. Rev. Lett. **80**, 936 (1998).
[50] S. K. Pampel, M. Marinelli, M. O. Brown, J. P. D'Incao, and C. A. Regal, Quantifying light-assisted collisions in optical tweezers across the hyperfine spectrum, arXiv:2408.15359.
[51] J. Ye, D. W. Vernooy, and H. J. Kimble, Trapping of single atoms in cavity qed, Phys. Rev. Lett. **83**, 4987 (1999).
[52] J. Kim, J. Lee, J. Han, and D. Cho, Optical dipole trap without inhomogeneous ac stark broadening, J. Korean Phys. Soc. **42**, 483 (2003).
[53] T. Yoon and M. Bajcsy, Laser-cooled cesium atoms confined with a magic-wavelength dipole trap inside a hollow-core photonic-bandgap fiber, Phys. Rev. A **99**, 023415 (2018).
[54] N. Schlosser, G. Reymond, I. Protsenko, and P. Grangier, Sub-poissonian loading of single atoms in a microscopic dipole trap, Nature (London) **411**, 1024 (2001).
[55] N. Schine, A. Ryou, A. Gromov, A. Sommer, and J. Simon, Synthetic Landau levels for photons, Nature (London) **534**, 671 (2016).
[56] L. W. Clark, N. Schine, C. Baum, N. Jia, and J. Simon, Observation of Laughlin states made of light, Nature (London) **582**, 41 (2020).
[57] H. Tanji-Suzuki, I. D. Leroux, M. H. Schleier-Smith, M. Cetina, A. T. Grier, J. Simon, and V. Vuletić, Chapter 4—Interaction between atomic ensembles and optical resonators: Classical description, Adv. At. Mol. Opt. Phys. **60**, 201 (2011).
[58] V. Vuletić, H. W. Chan, and A. T. Black, Three-dimensional cavity Doppler cooling and cavity sideband cooling by coherent scattering, Phys. Rev. A **64**, 033405 (2001).
[59] K. Murr, Large Velocity capture range and low temperatures with cavities, Phys. Rev. Lett. **96**, 253001 (2006).
[60] R. J. Schulze, C. Genes, and H. Ritsch, Optomechanical approach to cooling of small polarizable particles in a strongly pumped ring cavity, Phys. Rev. A **81**, 063820 (2010).
[61] V. Vuletić and S. Chu, Laser cooling of atoms, ions, or molecules by coherent scattering, Phys. Rev. Lett. **84**, 3787 (2000).
[62] See Supplemental Material at http://link.aps.org/supplemental/10.1103/941q-5sdq for additional details on ejection of atoms, detailed descriptions of the adaptive feedback protocol, cavity cooling mechanisms, collisional models for trapped atoms, and initial collisional analysis.
[63] P. Maunz, T. Puppe, I. Schuster, N. Syassen, P. W. Pinkse, and G. Rempe, Cavity cooling of a single atom, Nature (London) **428**, 50 (2004).
[64] P. Horak, G. Hechenblaikner, K. M. Gheri, H. Stecher, and H. Ritsch, Cavity-induced atom cooling in the strong coupling regime, Phys. Rev. Lett. **79**, 4974 (1997).
[65] P. Münstermann, T. Fischer, P. Maunz, P. W. H. Pinkse, and G. Rempe, Observation of cavity-mediated long-range light forces between strongly coupled atoms, Phys. Rev. Lett. **84**, 4068 (2000).
[66] P. Domokos, P. Horak, and H. Ritsch, Semiclassical theory of cavity-assisted atom cooling, J. Phys. B **34**, 187 (2001).
[67] J. Vaneecloo, S. Garcia, and A. Ourjoumtsev, Intracavity Rydberg superatom for optical quantum engineering: Coherent control, single-shot detection, and optical π phase shift, Phys. Rev. X **12**, 021034 (2022).
[68] M. Khudaverdyan, W. Alt, T. Kampschulte, S. Reick, A. Thobe, A. Widera, and D. Meschede, Quantum jumps and spin dynamics of interacting atoms in a strongly coupled atom-cavity system, Phys. Rev. Lett. **103**, 123006 (2009).
[69] M. O. Brown, T. Thiele, C. Kiehl, T.-W. Hsu, and C. A. Regal, Gray-molasses optical-tweezer loading: Controlling collisions for scaling atom-array assembly, Phys. Rev. X **9**, 011057 (2019).
[70] T. Grünzweig, A. Hilliard, M. McGovern, and M. F. Andersen, Near-deterministic preparation of a single atom in an optical microtrap, Nat. Phys. **6**, 951 (2010).
[71] Y. H. Fung and M. F. Andersen, Efficient collisional blockade loading of a single atom into a tight microtrap, New J. Phys. **17**, 073011 (2015).
[72] B. J. Lester, N. Luick, A. M. Kaufman, C. M. Reynolds, and C. A. Regal, Rapid production of uniformly filled arrays of neutral atoms, Phys. Rev. Lett. **115**, 073003 (2015).
[73] A. Lengwenus, J. Kruse, M. Volk, W. Ertmer, and G. Birkl, Coherent manipulation of atomic qubits in optical micropotentials, Appl. Phys. B **86** (2007).
[74] A. Fuhrmanek, R. Bourgain, Y. R. P. Sortais, and A. Browaeys, Free-space lossless state detection of a single trapped atom, Phys. Rev. Lett. **106**, 133003 (2011).
[75] M. P. A. Jones, J. Beugnon, A. Gaëtan, J. Zhang, G. Messin, A. Browaeys, and P. Grangier, Fast quantum state control of a single trapped neutral atom, Phys. Rev. A **75**, 040301(R) (2007).
[76] S. Kuhr, W. Alt, D. Schrader, I. Dotsenko, Y. Miroshnychenko, A. Rauschenbeutel, and D. Meschede, Analysis of dephasing mechanisms in a standing-wave dipole trap, Phys. Rev. A **72**, 023406 (2005).
[77] W. Xu, T. Šumarac, E. H. Qiu, M. L. Peters, S. H. Cantú, Z. Li, A. Menssen, M. D. Lukin, S. Colombo, and V. Vuletić, Bose-Einstein condensation by polarization gradient laser cooling, Phys. Rev. Lett. **132**, 233401 (2024).
[78] J. Duan, Z. Hu, X. Lu, L. Xiao, S. Jia, K. Mølmer, and Y. Xiao, Continuous field tracking with machine learning and steady state spin squeezing, Nat. Phys. **21**, 909 (2025).
[79] D. Shadmany, A. Kumar, A. Soper, L. Palm, C. Yin, H. Ando, B. Li, L. Taneja, M. Jaffe, D. Schuster, and J. Simon, Cavity qed in a high na resonator, arXiv:2407.04784.
[80] A. L. Shaw, A. Soper, D. Shadmany, A. Kumar, L. Palm, D.-Y. Koh, V. Kaxiras, L. Taneja, M. Jaffe, D. I. Schuster, and J. Simon, A cavity array microscope for parallel single-atom interfacing, arXiv:2506.10919.
[81] T. Kampschulte and J. H. Denschlag, Cavity-controlled formation of ultracold molecules, New J. Phys. **20**, 123015 (2018).
[82] K. Singh, C. E. Bradley, S. Anand, V. Ramesh, R. White, and H. Bernien, Mid-circuit correction of correlated phase errors using an array of spectator qubits, Science **380**, 1265 (2023).
[83] T. M. Graham, L. Phuttitarn, R. Chinnarasu, Y. Song, C. Poole, K. Jooya, J. Scott, A. Scott, P. Eichler, and

M. Saffman, Midcircuit measurements on a single-species neutral alkali atom quantum processor, Phys. Rev. X **13**, 041051 (2023).

[84] S. Ma, G. Liu, P. Peng, B. Zhang, S. Jandura, J. Claes, A. P. Burgers, G. Pupillo, S. Puri, and J. D. Thompson, High-fidelity gates and mid-circuit erasure conversion in an atomic qubit, Nature (London) **622**, 279 (2023).

[85] M. A. Norcia *et al.*, Midcircuit qubit measurement and rearrangement in a ^{171}Yb atomic array, Phys. Rev. X **13**, 041034 (2023).

[86] J. W. Lis, A. Senoo, W. F. McGrew, F. Rönchen, A. Jenkins, and A. M. Kaufman, Midcircuit operations using the *omg* architecture in neutral atom arrays, Phys. Rev. X **13**, 041035 (2023).